JOURNAL OF COMPUTATIONAL PHYSICS 77, 73–84 (1988)

Successive Embeddings of Excited Atomic Dipoles in Plasmas

G. NAOURI AND C. DEUTSCH

L.P.G.P., Bât. 212, Université Paris XI, 91405 Orsay Cedex, France*

AND

O. ATABEK AND R. LEFEBVRE

L.P.P.M., Bât. 212, Université Paris XI, 91405 Orsay Cedex, France*

Received October 13, 1986; revised April 1, 1987

An iterative and nonlinear procedure based on Renormalization group ideas is investigated for static screened Coulomb potentials through successive inclusion of excited 2-body orbitals. The key quantities are dielectric constants for every excited state, built into a hierarchy of nonlinear differential equations. Different numerical approaches to the Schrödinger problem are contrasted. They are implemented through the analytic solutions of the given HULTHEN potential. As a result, one observes a systematic shallowing of the pair interaction altogether with a blue shift of the bound–bound transitions.

I. INTRODUCTION

In several basic problems connected with pressure ionization and line broadening in strongly coupled plasma [1], one has to consider strongly overlapping electron-ion orbitals for the statically screened and 2-body interaction

$$\frac{e^{-r/D}}{r}, \tag{1}$$

with the Debye screening length

$$D=\left(\frac{k_B T}{4\pi e^2(n_e+Z^2 n_I+(Z-1)^2 n_{II})}\right)^{1/2}, \tag{2}$$

n_e = free electrons density, with n_I = density of fully stripped ions with charge Z, and n_I = density of hydrogenic ions with charge $Z-1$.

* Associé au C.N.R.S.

0021-9991/88 $3.00

Then, through powerful iterative schemes [2] afforded by the recently developed Renormalization-group methods, one can account for these messy entanglements by a systematic embedding of closed and excited orbitals pertaining to the potential (1). Thus, one has to consider a two-body Schrödinger problem solved numerically at every inclusion of a given excited orbital by the next excited one, and so on, up to the ionization limit which remains undisturbed throughout that process. The eigenquantities pertaining to the enclosed pair build up a smoothly space-varying dielectric function providing a kind of line screening to interaction (1), thus extended to

$$\frac{e^{-r/D}}{r\varepsilon(r)}. \tag{3}$$

A given excited orbital (n, l) labelled with usual hydrogenic quantum numbers n and l will thus experience a renormalized interaction (3) in lieu of the standard expression (1). The r-dependent dielectric function $\varepsilon(r)$ accounts for the enclosed dipoles arising from fast electrons orbiting on lower excited states with $n' \leqslant n$, $l' < l$. These latter belong to less excited electron-ion pairs.

Within this context, the main goal of the present work is to emphasize out the typical numerical technicalities involved with the implementation of the above renormalization group approach to pressure-induced shifts of bound levels in dense and hot plasmas. As far as we know, this is the first application of renormalization group techniques to atomic physics problems in dense plasmas.

II. Statement of the Problem and Formal Solution

The iterated embedding process is based on the crucial remark that radial wavefunctions $R_{nl}(r)$ for (n, l) states close to their ionization limit [9] can exhibit enormously enhanced spatial spreading, as compared to their nearly coulombic homologue $(D \to \infty)$.

The ionization limit of a Debye orbital is defined by the value $D_c(n, l)$ of the screening length which makes bound states (n, l) disappear into the continuum.

At this juncture, the salient is that for a D just above $D_c(n, l)$, $R_{nl}(r)$ displays a nearly horizontal r-derivative $dR_{nl}/dr \simeq 0$ for $r \geqslant a_0$ and also experiences a considerable delocalization by overlapping other wave functions pertaining to other ions with less excited electron-ion orbitals and smaller (n, l) values.

This crucial observation paves the way to a systematics of successive inclusions of lower excited orbitals within more excited ones. In the present approach, level excitations by collisions with plasma particles are already accounted for in Debye orbitals, and they are not expected to alter bound state trajectories any further.

In order to focus attention on dipole inclusions only, one has to consider the obvious monopole interactions (Coulomb repulsion) between ions as exactly balanced by a background of free electrons.

The formal procedure detailed elsewhere [1, 2] culminates into a succession of interrelated nonlinear differential equations for $Y_{nl}(r) = \beta e^2 \varepsilon_{nl}^{-1}(r)$. e denotes the electric charge; $\beta = (k_B T)^{-1}$ is the usual inverse thermal energy expressed in terms of the Boltzmann constant and the plasma temperature.

The key quantities $\varepsilon_{nl}(r)$ are then determined in a step-by-step procedure out of the eigenquantities $(E_{n'l'}, R_{n'l'}(r))$ pertaining to the lower enclosed dipole with quantum numbers (n', l'). The above-referenced hierarchy of nonlinear equations thus reads

$$dy_n(r) = -\tfrac{4}{3}\pi C \beta e^2 r^4 y_n^2(r) \sum_{\substack{n' < n \\ l' < l}} (2l' + l) \exp(-\beta E^0_{n'l'})\, R^2_{n'l'}(r)\, dr, \tag{4}$$

where

$$C = \tfrac{1}{2} n_e^2 (2\pi\hbar^2 / m_e k_B T)^{3/2}\, e^{\beta I}$$

depends on n_e, free electron number density in plasma, and I, ionization potential of a bound electron-ion pair in ground state. C expresses the SAHA equilibrium between free charges and bound excited states.

III. Numerical Procedure

The actual specificity of the renormalization group approach to pressure-induced shifts of bound levels in strongly coupled plasmas lies in the adequate combination of numerical techniques required to solve the nonlinear hierarchy (4) explained in more detail as

$$\begin{aligned}
&(\chi_{nl}(r) = r^2 R^2_{nl}(r)) \\
&\frac{dy_{2,0}(r)}{dr} = -C \frac{4\pi}{3} r^2 y^2_{2,0}(r)\, e^{-\beta E^0_{1s}} \chi^2_{1s}(r) \\
&\frac{dy_{2,1}(r)}{dr} = -C \frac{4\pi}{3} r^2 y^2_{2,1}(r)[e^{-\beta E^0_{1s}} \chi^2_{1s}(r) + 3\, e^{-\beta E^0_{2s}} \chi^2_{2s}(r)] \cdots
\end{aligned} \tag{4'}$$

with $y_{l,0}(r) \equiv 1$, expressing the ground state invariance throughout the whole renormalization procedure, which depends now entirely on the radial wave function $R_{nl}(r)$ of the Schrödinger problem with the interaction $Ze^{-r/D}/\varepsilon(r)$.

We found it especially convenient to solve numerically the nonlinear differential equations through the socalled RKV8 (Runge–Kutta of order 8) method developed by Werner [3].

That method, in contradistinction to the more standard version [4] of the Runge–Kutta algorithm is also able to treat accurately the case of exact quadratures.

Such capabilities are obviously required to process efficiently the classical limit ($l=0$ states) of Eqs. (4), i.e. (n_0 = average dipole density)

$$\frac{dy}{dr} = -\frac{16}{3} n_0 \pi^2 y^2 r^4 \exp[(y/r)(e^{-r/D} - e^{-r/\lambda})], \tag{5}$$

where $y' \to 0$ at the origin while $y \simeq (1/5\, Cr^5 + \text{const})^{-1}$ with $C = 16/3\pi n_0$ at infinity.

The Debye interaction (1) has been corrected for diffraction effects at $r \simeq 0$. These $\hbar \neq 0$ corrections thus provide a short-range regularization for the exponent in the r.h.s. of Eq. (5).

The merits of Werner's algorithm [3] are clearly appreciated when one recalls that an S-stage [4] $R-K$ formula is a scheme for calculating y_k from y_{k-1} using S function evaluations:

$$k_1 = f(x_{k-1}, y_{k-1}), \tag{6a}$$

$$k_i = f(x_{k-1} + a_i h_k, y_{k-1} + h_k \sum_{j=1}^{i-1} b_{ij} k_j), \qquad i = 2, ..., S, \tag{6b}$$

$$y_k = y_{k-1} + h_k \sum_{i=1}^{S} C_i k_i,$$

where $y(x_k; x_{k-1})$ is the solution of the local initial value problem $y'(t) = f(t, y(t))$ and $y(x_{k-1})$ while $h_k = x_k - x_{k-1}$ is the stepsize for step k.

The constants a_i, b_{ij}, and c_i define the method. They are tabulated in Werner's paper [3]. The method is of order p if p is the largest integer such that

$$\begin{aligned} T_k(h_k) &= [\, y(x_{k-1}, y_{k-1}) - y_k \,]\, h_k^{-1}, \\ &= 0(h_k^p) \end{aligned} \tag{7}$$

for any p times differentiable function $f(x, y)$.

More standard *RK* algorithms [4] provide for cases that reduce to quadratures (or others partially of this type as Eq. (5)) error estimates which are identically zero, and hence these estimates turn unreliable. Werner methods [3] are of arbitrarily high orders of accuracy. They provide matched results of successive order p and $p+1$ for which the total number of stage $\tilde{S}(p)$ remains reasonably small.

A pair of matched methods is denoted as an $(\tilde{S}(p), p(p+1))$-procedure.

IV. Numerov Versus Tridg

We found it convenient, for the purpose of numerical accuracy, nodes counting, and computing time saving, to work out the relevant eigenquantities from two related codes: TRIDG [5] and NUMEROV [6].

In the two methods $R_{nl}(r)$ is computed at $N+2$ equidistant points within interval $[R_0, R_{N+1}]$. A given R_i is defined by $R_i = R_0 + ih$, where $h = R_{N+1}/N+1$ and $R_0 = 0$.

The standard notations

$$P_i = P(R_i),\ V_i = V(R_i),\ P_i'' = \left.\frac{d^2P(R)}{dr^2}\right|_{R_i} \tag{8}$$

allow us to rewrite $(P(r) = R_{nl}(r))$

$$\left[\frac{d^2}{dr^2} + E - V(r)\right] P(r) = 0,$$
$$V(r) = -\frac{Z}{r} e^{-r/D} + \frac{l(l+1)}{r^2}, \tag{9}$$

as

$$P_i' = [V_i - E] P_i. \tag{10}$$

The expansion

$$P(R_i + h) = P(R_i) + hP_i' + \frac{h^2}{2!} P_i'' + \text{—}, \tag{11}$$

yields the usual finite difference approximation

$$h^2 P_i'' = P_{i+1} + P_{i-1} - 2P_i, \tag{12}$$

where $(h^4/12) P_i^{(4)}$ has been neglected out, which characterizes TRIDG [4].

For NUMEROV [6], one makes use of

$$h^2 P_i'' = Y_{i+1} + Y_{i-1} - 2Y_i$$
$$Y_i = P_i - \frac{h^2}{12} P_i'' \tag{13}$$

with first neglected term $(H^6/240) P_i^{(6)}$.

The boundary conditions are taken as

$$\text{TRIDG} \begin{cases} P(R_0) = 0 \\ P(R_N) = 0 \end{cases}$$

$$\text{NUMEROV approximate } \lim_{r \to 0} R_{nl}(r)$$

$$\lim_{r \to \infty} R_{nl}(r),$$

$P(r)$ is propagated simultaneously inward and outward from R_N and R_0. Matching is achieved at $R = R_M$ where one imposes $P_M = 1$.

Normalization results from

$$\left[\sum_{i=1}^{N} P_i^2 + \frac{P_0^2}{2} + \frac{P_{N+1}^2}{2}\right] h = 1, \tag{14}$$

R_M is determined, in both methods, as a classical turning point fulfilling $V(R_M) = E'$, an a priori energy estimate.

According to *WKB* theory, the wave function does no longer oscillate beyond R_M. Therefore, counting the number of nodes in the $[R_0, R_M]$ interval allows an easy check of the level labelling. Also, the choice $R_N = 10R_M$ is sufficient to secure a nearly complete damping of $P(r)$ at the end of a range with a reasonable extension and constant mesh.

It is also important to notice that the approximate $P(R)$ required to implement NUMEROV as well as the initial guess E' are deduced from the corresponding eigenquantities for the Hulthen potential [7, 8]

$$\frac{e^2}{\varepsilon(r)} \frac{\alpha e^{-\alpha r}}{(1 - e^{-\alpha r})}, \qquad \alpha = D^{-1}$$

conveniently analyzed under the form ($\delta = \alpha a_0$)

$$E_n = +\tfrac{1}{2} a_n^2 \delta^2, \qquad \chi_n(r) = e^{-a_n \delta r} \phi_n(r)$$

amenable, up to a certain extent, to an exact analytic treatment.

In this way, one easily obtains a good start for the Debye eigenquantities.

(A) *TRIDG*

Combining Eqs. (10) and (12) one has to solve

$$[P_{i+1} - 2 - h^2 V_i] P_i + P_{i-1} = -h^2 E P_i, \tag{15}$$

where $P_0 = 0$ and $P_{N+1} = 0$, other P's are deduced from

$$\underbrace{\begin{bmatrix} -[2 + h^2 V_1] & 1 & & \\ 1 & -[2 + h^2 V_2] & 1 & 0 \\ & \ddots & \ddots & \ddots \\ 0 & & 1 & -[2 + h^2 V_N] \end{bmatrix}}_{A} \underbrace{\begin{bmatrix} P_1 \\ \vdots \\ P_N \end{bmatrix}}_{\mathbf{P}} = -h^2 E \begin{bmatrix} P_1 \\ \vdots \\ P_N \end{bmatrix} \tag{16}$$

diagonalized through the Rutishauser [10] method, with eigenvalues appearing in order of increasing modulus, which allows us to restrict our focus to a few of them.

Eigenvectors are worked out through a method designed by two of us (O.A. and R.L.) for any tridiagonal matrix with the lower diagonal containing only unit entries. From (λ = any eigenvalue)

$$\begin{pmatrix} a_1-\lambda & b_1 & 0 & 0 & \cdots \\ 1 & a_2-\lambda & b_2 & 0 & \cdots \\ 0 & 1 & a_3-\lambda & b_3 & \cdots \\ & & & 0 & a_N-\lambda \end{pmatrix} \begin{pmatrix} P_1 \\ \vdots \\ P_N \end{pmatrix} = 0, \tag{17}$$

one gets

$$P_i = \alpha_i P_{i+1} \qquad \text{with} \quad \alpha_i = \frac{-b_i}{(a_i-\lambda)+\alpha_{i-1}}. \tag{18}$$

First Eq. (18) yields $\alpha_1 = -b_1/(a_1-\lambda)$; all the other α_1 follow by induction for $i \in [1, M]$. Inward propagation gives

$$P_i = \alpha_i P_M \qquad \text{with} \quad \alpha_i = \sum_{j=i}^{M-1} \alpha_j,$$

putting $p_M = 1$ determines P_i, $i \in [1, M]$.

The $P(r)$ nodes are thus counted by the number of $\alpha_i < 0$.

For P_i with $i \in [M, N]$ outward propagation gives

$$P_i = \gamma_i P_M \qquad \text{with} \quad \gamma_i = \frac{(a_{i-1}-\lambda)\gamma_{i-1}+\gamma_{i-2}}{-b_{i-1}}, \tag{19}$$

where the process is initialized through

$$\gamma_{M+1} = \frac{a_M - \lambda + \alpha_{M-1}}{-b_M} \qquad \gamma_{M+2} = \frac{(a_{M+1}-\lambda)\gamma_{M+1}+1}{-b_{M+1}}.$$

There are $n-l$ oscillations of $P(R)$ within $[0, R_M]$. Taking 40 points/oscillation, we are led to work with $M = 40\ (n-1)$ and $N = 10M$, which allowed us to retrieve Hulthen wave functions with a 10^{-3} accuracy.

(B) *NUMEROV*

From Eqs. (10) and (13′) one derives

$$-h^{-2}Y_{i-1} + \alpha_i Y_i - h^{-2}Y_{i+1} = 0, \tag{20}$$

with $\alpha_i = 2h^{-2} + (V_i - E)[1 - (h^2/12)(V_i - E)]^{-1}$. Setting

$$Y_0 = 0 \qquad Y_N \cong Y_{N-1}$$

$$\alpha_N = h^{-2} + (V_N - E)\left[1 - \left(\frac{h^2}{12}\right)(V_N - E)\right]^{-1}$$

one gets the matricial equality

$$M\mathbf{Y}=0 \qquad \text{with} \quad \mathbf{Y}=\begin{pmatrix} Y_1 \\ \vdots \\ Y_M \\ \vdots \\ Y_N \end{pmatrix}$$

and

$$M=\begin{pmatrix} \alpha_1 & -h^{-2} & 0 & \cdots & 0 \\ -h^{-2} & \alpha_2 & 0 & \cdots & 0 \\ 0 & -h^{-2} & \alpha_3 & 0\cdots & 0 \\ \vdots & \vdots & \vdots & & \vdots \\ \vdots & \vdots & \vdots & & 0 \\ 0 & 0 & 0 & -h^{-2} & \alpha_N \end{pmatrix}. \tag{21}$$

Solutions are propagated from both ends towards R_M.

Starting with a Hulthenlike trial eigenenergy $\varepsilon = E - dE$, one gets

$$F(\varepsilon)=F(E)-dEF'(\varepsilon)\rightarrow dE=-\frac{F(\varepsilon)}{F'(\varepsilon)}, \tag{22}$$

where $F(E)=-h^{-2}Y_{M-1}+\alpha_M Y_M - h^{-2}Y_{M+1}$ is identically zero when $dE=0$. From Eq. (21), one obtains

$$F'(\varepsilon)=\sum_{i=1}^{N} Y_i^2 \frac{\partial \alpha_i}{\partial \varepsilon}, \tag{23}$$

where $(\partial\alpha_i/\partial\varepsilon)=-[1-(h^2/12)(V_i-\varepsilon)]^{-2}\rightarrow Y_i^2(\partial\alpha_i/\partial\varepsilon)=P_i^2$ and finally

$$dE=[h^{-2}(-Y_{M-1}+2Y_M-Y_{M+1})+(V_M-\varepsilon)P_M]\Big/\sum_{i=1}^{N}(-P_i^2).$$

NUMEROV thus allows for a 10^{-6} accuracy on eigenvalues.

V. Results and Discussion

In Fig. 1 one observes the inverse dielectric function $Y_{nl}(r)=\varepsilon_{nl}^{-1}(r)$ with averaged out l dependence, for $1\leqslant Z\leqslant 6$ and different (D, Λ_e) values. Λ_e is the electron plasma parameter $(\beta=(k_B T)^{-1})$

$$\Lambda_e=\frac{\beta e^2}{D_e}=\frac{2.43\times 10^{-4} n_e(\mathrm{cm}^{-3})^{1/2}}{T(^\circ\mathrm{K})^{3/2}} \tag{24}$$

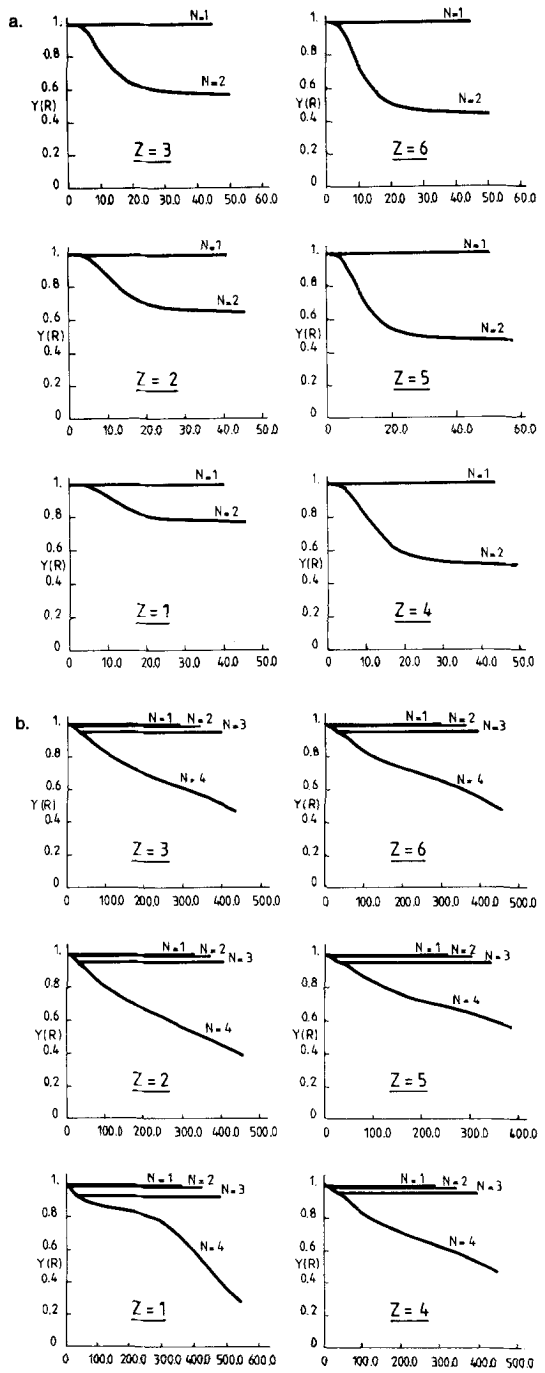

FIG. 1. $Y_{nl}(r) = 1/\varepsilon_{nl}(r)$ as a function of ionic radii a_0/Z for $1 \leqslant Z \leqslant 6$ and various plasma conditions. (a) $D = 5a_0/Z$, $\Lambda_e = 0.4$. (b) $D = 15a_0/Z$, $\Lambda_e = 0.7$.

in terms of the electron screening length D_e, obtained by putting $n_I = n_{II} = 0$ in Eq. (2).

Larger D allows for more renormalized bound states, within the Debye ($\varepsilon(r) \equiv 1$) spectrum, left unchanged through the present procedure. The embedding process does not modify the ionization limit. It can then be considered as a very soft effect, which does not participate to the well-known and first-order orbital overlap leading to pressure ionization. $Y_{nl}(r)$ essentially acts as a prefactor within a generalized Debyelike interaction. In agreement with Eqs. (4)–(4'), $Y_{nl}(r)$ goes ultimately down to zero, at a Zr/a_0 distance, located beyond the abscissa in Fig. 1.

In this work, we restrict our focus to small Z, because in the opposite $Z \to \infty$ limit, Debyelike wave functions become too hydrogenic, and do not exhibit any sensitive delocalization effect.

According to Iafrate and Mendelsohn [11] pseudo-analytic estimates,

$$R_{nl}(r) \sim e^{-ZS(r)} \sum_{m=0}^{\infty} a_m(r)\, Z^{-m}, \qquad Z \to \infty \tag{25}$$

$$R_{nn-1}(r) \sim r^{n-1}\, e^{-(Zr/n)+\psi(r)} \left(1 + \frac{f(n, D, r)}{Z}\right) \tag{25'}$$

$$\psi(r) = n \sum_{i=1}^{\infty} \frac{(-r/D)^i}{ii!}.$$

The nucleus has turned too attractive in this limit. The resulting $R_{nl}(r)$ gets shrinked on it, and the potentiality of successive embeddings of excited orbitals is then gradually lost as Z increases. On the other hand, one might argue that non-hydrogenic orbitals behave differently in the same $Z \to \infty$ limit. We are currently exploring a Thomas–Fermilike modelization of the electron-ion interaction under the form [12]

$$V(r) = \frac{2}{r}\,[N\gamma(r) - 2], \tag{26}$$

where $N =$ number of bound electrons $- 1$,

$$\gamma(r) = \frac{HY}{H+1}, \qquad Y = e^{r/d} - 1, \qquad 0.5 < \frac{d}{a_0} < 1.3$$

$$H = \frac{d}{a_0}\, N^{0.4}.$$

A more global feeling about the whole process is afforded by a three dimensional plot (Fig. 2) of the wavelength relative shifts $-\Delta\lambda/\lambda$ as a function of Z and Λ_e.

Blue relative shifts $> 10^{-3}$ are obtained with respect to the Debye ones. They are distinctly larger than those usually observed in weakly coupled plasma ($\Lambda_e < 0.1$). These latter are triggered by other temperature-dependent mechanisms.

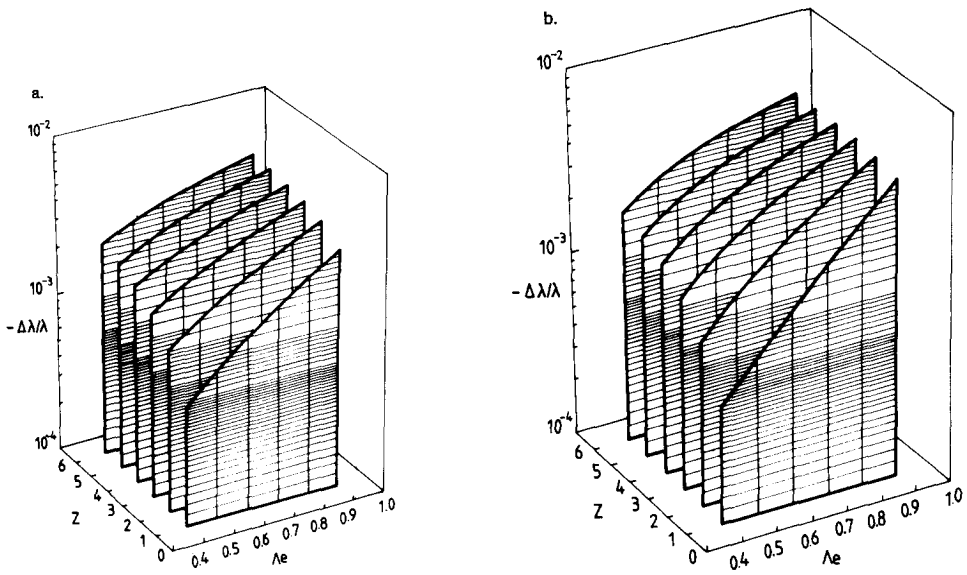

FIG. 2. Relative wavelength shifts with respect to the Debye ones ($\varepsilon(r) = 1$) for various conditions as a function of Z and Λ_e. (a) Ly_α and $D = 5a_0/Z$. (b) Ly_α and $D = 7a_0/Z$.

The present Ly_α and Ly_β shifts steadily increase with Z in the hydrogenic sequence, and also with Λ_e, up to the optimum Λ_e for which the last bound state desappears into the continuum.

These negative shifts, with respect to the usual unrenormalized Debye ($\varepsilon(r) \equiv 1$) transitions, act to reduce the overall Debye red shift. An effect increasing with Z and Λ_e, which thus contributes to reducing the Debye red shifts usually recognized as too large.

Finally, we have to comment on the use of a pure electron plasma parameter Λ_e (Eq. (24)) in lieu of the full $\Lambda = \beta e^2 D^{-1}$.

Λ_e enhances $-\Delta\lambda/\lambda$. Also, in many practical cases, we are likely to handle situations with $T_e > T_i$, where electrons display more capabilities [13] for long range screening than those expected from far distant ions, not involved in the present renormalizing procedure.

To summarize our findings, we started with the observation that the radial wave function of a given Debye bound state, close to its ionization limit ($D \sim D_c(n, l)$) extends over many interionic distances. We worked out iterative embeddings of orbitals with increasing excitation, by using a three dimensional quantum-mechanical extension of the two dimensional KT classical procedure [2]. As a result, we got blue pressure-induced shifts with respect to the usual Debye ones for hydrogenic ions in strongly coupled plasmas.

ACKNOWLEDGMENT

One of us (G.N.) is deeply endebted to Professor A.J. Alcock for giving him access to the NRC computing facilities.

REFERENCES

1. C. DEUTSCH AND G. NAOURI, *Phys. Lett. A* **111**, 54 (1985); C. DEUTSCH AND S. DONIACH, *Phys. Rev. B* **29**, 2724 (1984) for a two-dimensional approach; C. DEUTSCH AND G. NAOURI, *Phys. Rev. B* (to be published).
2. J. M. KOSTERLITZ AND D. J. THOULESS, *J. Phys. C* **6**, 1181 (1973); K. G. WILSON, *Rev. Mod. Phys.* **55**, 583 (1983).
3. J. H. WERNER, *SIAM J. Numer. Anal.* **15**, 772 (1978).
4. K. R. JACKSON, W. H. ENRIGHT, AND T. E. HULL, *SIAM J. Numer. Anal.* **15**, 615 (1978); D. SANCHEZ, R. C. ALLEN, JR., AND W. T. KYSNER, *Differential Equations* (Addison–Wesley, Reading, MA 1983).
5. D. G. TRUHLAR, *J. Comput. Phys.* **10**, 123 (1972).
6. J. W. COOLEY, *Math. Comput.* **15**, 363 (1961).
7. C. S. LAM AND Y. P. VARSHNI, *Phys. Rev. A* **4**, 1875 (1971).
8. R. L. GREENE AND C. ALDRICH, *Phys. Rev. A* **17**, 795 (1978).
9. N. GRANDJOUAN AND C. DEUTSCH, *Phys. Rev. A* **17**, 795 (1978).
10. E. DURAND, *Solutions numériques des équations algébriques*, T.2 (Masson, Paris, 1972), p. 281.
11. G. J. IAFRATE AND L. B. MENDELSOHN, *Phys. Rev.* **182**, 244 (1969).
12. A. E. S. GREEN, D. L. SELLIN, AND A. S. ZACHOR, *Phys. Rev.* **184**, 1 (1969).
13. N. A. KRALL AND A. W. TRIVELPIECE, *Principles of Plasma Physics*, (McGraw–Hill, New York, 1978), Chap. 11.